7218 *Biochemistry* **2010,** *49,* 7218–7226
DOI: 10.1021/bi1008112

BIOCHEMISTRY
including biophysical chemistry & molecular biology
Article

Product Analysis and Inhibition Studies of a Causative Asn to Ser Variant of 4-Hydroxyphenylpyruvate Dioxygenase Suggest a Simple Route to the Treatment of Hawkinsinuria[†]

June M. Brownlee, Brian Heinz, Judith Bates, and Graham R. Moran*

Department of Chemistry and Biochemistry, University of Wisconsin—Milwaukee, 3210 North Cramer Street, Milwaukee, Wisconsin 53211-3029

Received May 20, 2010; Revised Manuscript Received July 12, 2010

ABSTRACT: Hawkinsinuria is a severe inherited condition that has a significant impact on the health of infants. The disease manifests as metabolic acidosis that significantly slows the growth rate and induces persistent diarrhea and vomiting. Though other causes may exist, an autosomal dominant mutation that alters codon 241 of the 4-hydroxyphenylpyruvate dioxygenase (HPPD) gene from encoding an asparagine to encoding a serine gives rise to the symptoms of the disease. The observed pattern of dominance of this mutation belies the paucity of reports of this disease in the literature and suggests that it may be rarely diagnosed. Diagnosis is based on the presence of 2-amino-3-{[2-(carboxymethyl)-2,5-dihydroxy-1-cyclohex-3-enyl]sulfanyl}propanoic acid (hawkinsin) in the urine. We have made the structurally equivalent mutation in the *Streptomyces avermitilis* (N245S) and rat (N241S) genes and shown that in both cases the N to S variant enzyme forms quinolacetic acid in place of the native product 2,5-dihydroxyphenylacetic acid (homogentisate). Importantly, the variant enzyme is highly active, establishing the basis for dominant pedigree pattern. Quinolacetic acid reacts readily by Michael addition with cellular thiols to form a two-electron oxidized form of hawkinsin. The N to S variants are also susceptible to inhibition by 2-[2-nitro-4-(trifluoromethyl)benzoyl]-1,3-cyclohexanedione (NTBC), a known inhibitor of wild-type HPPD. NTBC has been approved for use in the treatment of type I tyrosinemia and as such has an extensive history of use with infants. The N to S variant undergoes an apparent three-step binding mechanism with NTBC that forms with rate constants similar to those observed for the wild-type enzyme. Moreover, the extreme stability of the HPPD·NTBC complex suggests that NTBC would be a potent therapeutic for Hawkinisinuria that would alleviate the extreme frailty experienced in the early life period.

Tyrosine catabolism is an ancient pathway common to ostensibly all aerobes. It is comprised of five enzymatic activities that collectively transform tyrosine to the organic acids acetoacetate and fumarate. These products are energy yielding and define the core purpose of the pathway. However, each kingdom of life has adapted the pathway to unique other purposes. Bacteria draw off intermediate metabolites to synthesize antibiotic substructures, cofactors, and melanins. The pathway is essential in plants that use it to form plastoquinone and tocopherol. In mammals, the catabolism of tyrosine is used to control concentrations of this sparingly soluble amino acid in the blood. In humans, defects in the genes that encode the enzymes of the pathway lead to five metabolic disease states (*1*). 4-Hydroxyphenylpyruvate dioxygenase (HPPD)[1] catalyzes the second step in this pathway, transforming 4-hydroxyphenylpyruvate (HPP) to homogentisate (HG). Mutations to the gene encoding this enzyme are understood to give rise to two of the five metabolic disorders, type III tyrosinaemia and Hawkinsinuria. In the former, the HPPD gene product is noncatalytic, while in the case of Hawkinsinuria, the HPPD variant consumes the substrate but appears abortive, yielding an alternative product that is reactive and known to form a covalent adduct with cellular thiols.

Hawkinsinuria was first described in the literature in the 1970s, and as early as 1977, it was realized that a HPPD defect was involved in the pathology (*2*). Hawkinsinuria has been reported a handful of times since, with occurrences in Australia, Europe, India, and North America (*3*−*7*). Its apparent infrequency notwithstanding, Hawkinsinuria is a weakening condition, causing afflicted infants to suffer persistent acidosis accompanied by vomiting and diarrhea and to fall severely behind their cohort in growth rate. Additionally, hair growth abnormalities and liver enlargement can result (*8*). The reported onset of symptoms often accompanies weaning and may be ameliorated by a low-protein or tyrosine-restricted diet (*6*, *9*, *10*). Interestingly, the symptoms abate as the individual passes out of infancy.

The hallmark of this disease state is the presence of the eponymous sulfur-containing amino acid, hawkinsin, in the urine (Scheme 1). This molecule (2-amino-3-{[2-(carboxymethyl)-2,5-dihydroxy-1-cyclohex-3-enyl]sulfanyl}propanoic acid) derives its name from the surname of the first patient described in the literature and was shown by isotope tracking to be a tyrosine metabolite (*11*). Other unusual metabolites are excreted by Hawkinsinuria sufferers, including 4-hydroxyphenyllactic acid, 4-hydroxyphenylacetic acid (HPA), 4-hydroxycyclohexylacetic

[†]This research was supported a National Science Foundation grant to G.R.M. (MCB0843619) and by a University of Wisconsin—Milwaukee Research Growth Initiative Grant to G.R.M.

*To whom correspondence should be addressed. Phone: (414) 229-5031. Fax: (414) 229-5530. E-mail: moran@uwm.edu.

[1]Abbreviations: HPPD, 4-hydroxyphenylpyruvate dioxygenase; HPP, 4-hydroxyphenylpyruvate; NTBC, 2-[2-nitro-4-(trifluoromethyl)benzoyl]-1,3-cyclohexanedione; HG, homogentisate; QAA, quionolacetic acid; IPTG, isopropyl β-thiogalactopyranoside; HPLC, high-pressure liquid chromatography; LC−MS, liquid chromatographic separation coupled to mass spectrometric detection; WT, wild type; NMR, nuclear magenetic resonance.

 Published on Web 07/13/2010

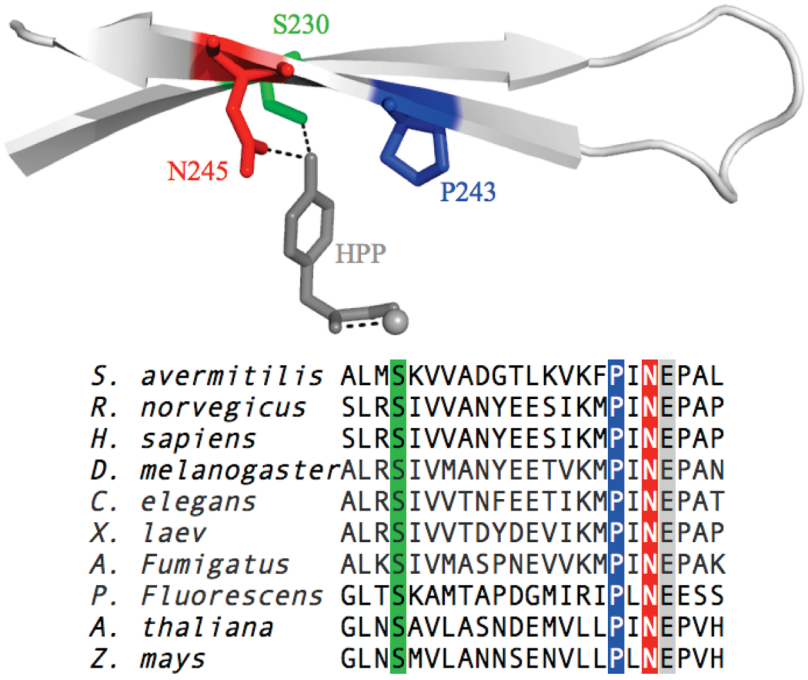

FIGURE 1: Conservation of the asparagine that is altered to serine in Hawkinsinuria patients. This residue is on the fourth β-strand of the β-barrel common to all vicinal oxygen chelate enzymes. The putative 4-hydroxyphenylpyuvate binding site was modeled in earlier work using molecular dynamics and was based the observed binding position for hydroxymandelate in the closely related enzyme hydroxymandelate synthase. In this position, the 4-hydroxyl of the substrate phenol is within hydrogen bonding distance of the asparagine in question and a conserved serine residue. A nearby conserved proline residue is shown to give context to parts of Discussion and Scheme 2.

Scheme 1

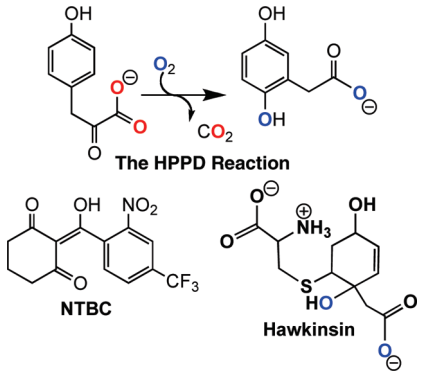

acid (4-HCAA), 5-oxoproline, and quinolacetic acid (QAA), with 4-HCAA predominating postinfancy.

Until recently, a causative mutation for Hawkinsinuria was not known. The disease had been shown to follow an autosomal dominant pattern of inheritance (belying the relative paucity of case studies in the literature) (*5*), and DNA sequencing from an Australian and an American patient a decade ago had lead to the conclusion that the causative mutation was in a region of the gene that would result in an N-terminal defect in the protein (A33T) (*10*); however, it was subsequently shown that this was a frequent polymorphism and not the causative mutation (*12*) (vide infra). It has also been suggested that hawkinsin may arise from intestinal flora that harbor a causative mutation in the HPPD gene (*2*). Recently, a case has emerged in which the individual presented as having Hawkinsinuria but was found to be compound heterozygous, with an inactive (type III tyrosinemia) allele, and a previously unreported missense mutation in the other allele, encoding an Asn to Ser switch (*7*). The N241S mutation was therefore presumed to be causative for Hawkinsinuria.

Asparagine 241 is conserved in all known HPPD sequences (~500) (Figure 1). HPPD variants at this position have been studied in the context of bacterial HPPD enzymes and range from seriously impaired (*13*) to "wild-type-like" (*14*). However, the mutation to serine was not among the variants reported. We report here on the in vitro study of the positionally equivalent N to S variants in the contexts of the *Streptomyces avermitilis* (SaHPPD) and *Rattus norvegicus* (RnHPPD) HPPD enzymes. We show that the predominant product of this variant is the reactive dienone, QAA, in place of the normal product HG (Schemes 1 and 2). As previously reported for the synthesis of hawkinsin, QAA is susceptible to the formation of thiol conjugates by Michael addition that, in turn, could readily give rise to hawkinsin (Scheme 1) (*2*). Such conjugates would be expected to form from glutathione-mediated detoxification reactions (*2*, *13*). Further, we show that the *S. avermitilis* N245S and rat N241S variants, like wild-type HPPD, are susceptible to 2-[2-nitro-4-(trifluoromethyl)benzoyl]-1,3-cyclohexanedione (NTBC) inhibition (Scheme 1). NTBC (also known as Nitisinone or Orfadin) was developed originally as an herbicide that is able to halt the production of plastoquinone, and molecules of its type are in worldwide use against broadleaf plants (*15*−*18*). The prolonged half-life of NTBC in mammalian metabolism (~54 h) undermined its perceived value as an herbicide. However, this characteristic has since made it a highly effective drug (*19*), approved for the treatment of the otherwise lethal disease type I tyrosinemia (*20*). NTBC has also been suggested for use with alkaptonuria (*21*), and the data presented here suggest NTBC as a therapeutic for Hawkinsinuria for use during the early life, symptomatic period.

MATERIALS AND METHODS

Materials. NTBC was provided as a gift from Swedish Orphan AB. HPP and HG were purchased from Acros Chemicals. Competent BL21(DE3) *Escherichia coli* cells were obtained

from Invitrogen. IPTG was from Gold Biochemicals. D_2O was from Cambridge Isotope Laboratories. Q-Sepharose was from Bio-Rad. Sephacryl S-200 was obtained from Amersham. All other chemicals, buffers, and biological media were obtained from Fisher Scientific or Sigma-Aldrich Chemicals and were of the highest purity available.

Mutagenesis. pET17b-derived (Novagen) plasmids carrying the *R. norvegicus* (pRNHPPD)and *S. avermitilis* (pSAHPPD) HPPD genes were mutated using the Stratagene QuikChange Lightning kit. Mutagenic oligonucleotides also encoded silent mutations for screening purposes that introduced an MscI site in the case of the *S. avermitilis* gene and a NarI site for the *R. norvegicus* gene. The following oligonucleotides and their respective reverse complement oligonucleotide were used to mutate the HPPD gene(s): *R. norvegicus*, CATCAAAATGCCCATTA***G***T-GAACCGGC**G**CCGGGCAGG; and *S. avermitilis*, GTCA-AGTTCCCGATCA***G***CGAGCCCGCCC**T**GGCCAAGAAGA-AGTCCC. For each, the change encoding serine is shown in bold and italics and the change introducing the restriction site is in bold with the restriction site underlined. Plasmids showing the expected digestion pattern were sequenced in the region of the HPPD gene to confirm the desired mutations and the absence of additional spurious mutations (Sequetech, Mountainview, CA).

Expression and Purification. The *S. avermitilis* HPPD N245S mutant plasmid, pSAHPPDN245S, was first transformed into BL21(DE3) *E. coli* cells. The protein was then expressed and purified as previously detailed for the WT enzyme (*22*). Briefly, cells were harvested 2.5 h after IPTG induction, frozen, thawed, resuspended in buffer, and disrupted by sonication. Supernatants of the sonicate were treated with streptomycin sulfate and then fractionated with ammonium sulfate to yield the 45−65% saturation fraction. This was then dissolved and chromatographed using successive Q Sepharose anion exchange and Sephacryl S-200 size exclusion. Solutions of the purified protein could be stored at −80 °C without loss of activity upon thawing.

Expression and preparation of crude wild-type and N241S variant *R. norvegicus* HPPD were achieved via transformation of the pET-17b-derived *R. norvegicus* HPPD plasmid, pRNH-PPDN241S, into BL21 (DE3) *E. coli* cells. These cells were then spread on LB agar plates containing 100 μg/mL ampicillin and allowed to grow at 37 °C for 12 h. The lawns of cells on the plates were then resuspended using LB broth to create an innoculum. One liter cultures of LB broth with ampicillin (100 μg/mL) were allowed to grow at 28 °C with shaking at 250 rpm for 12 h. Cells were harvested by centrifugation with a Sorval RC-3C centrifuge at 4700*g* for 30 min at 4 °C. Cell pellets were then resuspended in 20 mM HEPES (20 mL/L of culture), 1 mM EDTA buffer at pH 7.0 and sonicated on ice using a Branson model 450 sonifier fitted with a blunt tungsten tip (6 × 1 min at 40 W), ensuring the temperature did not exceed 10 °C. All remaining steps were conducted at 4 °C. The sonicated slurry was centrifuged at 32800*g* for 30 min. Streptomycin sulfate was added to the supernatant to a final concentration of 1.5% (w/v) and stirred for 10 min. This solution was then centrifuged at 19700*g* for 15 min. A 2 mL aliquot of the streptomycin-treated supernatant was added to 13 mL of 10 mM phosphate buffer (pH 7.0) and concentrated using a prerinsed Amicon Ultra centrifugal (nominal molecular mass limit of 10 kDa) filter by centrifugation at 2400*g* for 45 min. The retentate was then resuspended in 16 mL of the phosphate buffer and centrifuged again for 40 min. The retentate was then brought to a final volume of 1 mL with the phosphate buffer, and this preparation was used for all consecutive experiments. The sample was estimated by PAGE to contain ~60% RnHPPD.

Kinetic Analysis. The activity of the SaHPPD N245S protein was observed as the consumption of molecular oxygen in the presence of HPP using a Hansatech Oxygraph dioxygen electrode. The standard assay was undertaken at 25 °C and comprised of 10 μM ferrous sulfate, 200−300 nM HPPD, 2 mM ascorbate, ~250 μM O_2, and varying levels of HPP in HEPES buffer (pH 7.0). The enzymatic reaction was initiated by HPP addition after all other components were added. Background rates of oxygen consumption due to Fenton chemistry were assessed prior to the addition of HPP, and these rates were subtracted from the initial steady state reaction rates reported. For reactions in which the concentration of molecular oxygen was varied, the initial concentration was established by passing a mixture of N_2 and O_2 gas supplied by a Maxtec Maxblend gas blender across the surface of the reaction solution within the electrode reaction vessel for 10 min prior to initiation of the assay.

Product Analysis. To establish what product(s) was being made by the N to S HPPD variants, the reaction product was prepared in milligram quantities, purified, and studied by NMR. For these reactions, the standard assay conditions as described above were used with the exception of the reaction being undertaken in 50 mM sodium phosphate buffer (pH 7.0) and with 10 μM enzyme. After 200 μM dioxygen had been consumed in response to the addition of 200 μM HPP, the Oxygraph reaction cell was opened to air and O_2 equilibrium was re-established, at which time additional 200 μM HPP was added and an equivalent concentration of dioxygen consumed. This procedure was repeated according to the desired yield of product. The contents of the Oxygraph cell were then removed, and the mixture was separated using HPLC. The sample was prepared for chromatographic separation by solid phase extraction using Waters, Sep-Pak cartridges. This involved binding to the solid phase in aqueous reaction buffer, washing with water, and eluting with acetonitrile. The products were then dried under vacuum, dissolved in 10 mM sodium phosphate (pH 7.0), and chromatographed using a Waters 600E HPLC system fitted with a 21.2 mm × 250 mm Synergi 10 μm polar-RP Phenyl column (Phenomenex). The column was run under isocratic conditions at 4 mL/min with a mobile phase consisting of 10 mM sodium phosphate (pH 7.0) and 1% acetonitrile. Elution was monitored at 220 and 276 nm using a Waters 2487 dual absorbance detector. The product was collected, frozen with dry ice, and lyophilized. It was then dissolved in 99.9% D_2O or a 5% D_2O/95% H_2O mixture. One-dimensional (1D) ^1H spectra were recorded on a 300 or 500 MHz Bruker NMR instrument. For the 95% H_2O samples, the water signal was suppressed with the WATERGATE pulse sequence using a τ of 200 μs. ^{13}C and two-dimensional experiments were undertaken on the 500 MHz instrument using respective broadband observe and broadband inverse probes.

Spectrophotometric changes associated with the catalytic activity of the *S. avermitilis* N245S mutant protein (SaHPPD N245S) were observed to reaffirm that the product formed was not the native product. The reaction mixture included 120 μM HPP, 20 μM Fe(II), and either 3.5 μM SaHPPD N245S or 4.2 μM wild-type SaHPPD in 50 mM sodium phosphate buffer (pH 7.0). A Hewlett-Packard 8453 diode array spectrophotometer was used initially to record a baseline with all reaction components excluding HPP. The reaction was then initiated with HPP and the mixture incubated for 4 min before an end point spectrum was recorded and verified. To account for spectrophotometric changes that are not a result of the evolution of product, the identical protein/Fe(II) mixtures were

followed for an equivalent time in the absence of HPP, and the spectra of those controls were also recorded. The final control reaction spectra were then subtracted from the final enzymatic reaction spectra, and the results were compared to the spectrum of HPP alone recorded under the same buffer conditions.

The coupling of HPP consumption to oxygen consumption and product formation with the SaHPPD N245S and RnHPPD N241S variants was evaluated in defining the efficiency of the observed product formation. Enzymatic reaction mixtures containing known limiting amounts of HPP were evaluated using a combination of oxygen electrode end point assays and analytical HPLC. For both WT and variant forms of each enzyme, the assay included either 50 μM purified enzyme (*S. avermitilis* enzymes) or 75 μL of the crude enzyme extract (*R. norvegicus* enzymes), 20 μM ferrous sulfate, and 100 μM HPP in 10 mM phosphate buffer (pH 7) at 25 °C. For each reaction, a control aliquot, representing the composition of the reaction before initiation, was removed prior to the addition of HPP. After the addition of HPP, the reaction was allowed to proceed until the rate of consumption of dioxygen returned to that of the observed background rate due to Fenton chemistry. The control and turnover samples were then filtered using a 0.5 mL Amicon (10 kDa nominal molecular mass limit) centrifugal ultrafiltration device. Twenty microliters of each sample was then subjected to analytical HPLC using a Waters 600E HPLC system coupled to a 4.6 mm × 250 mm Synergi 10 μm polar-RP Phenyl column (Phenomenex) run under isocratic conditions at 1 mL/min with a mobile phase consisting of 10 mM sodium phosphate (pH 7.0) and 0.5% acetonitrile. Elution was monitored at 220 and 276 nm using a Waters 2487 dual absorbance detector.

Coupling of Quinolacetic Acid to Thiols. Approximately equimolar amounts of cysteine and QAA were reacted to formally show the formation of a hawkinsin-like product from the N to S variant reaction product. This reaction was initiated under anaerobic conditions to avoid oxidative production of cystine. The reactants were prepared in 10 mM sodium phosphate buffer (pH 7.4), and each was placed in a side arm of an anaerobic cuvette. Buffer [800 μL of 10 mM sodium phosphate (pH 7.4)] was added to the cuvette to establish a spectrophotometric baseline prior to the reaction. The cuvette was then sealed and subjected to 45 alternating cycles of vacuum and argon. QAA (320 μL of a 4.58 mM solution) was then mixed with cysteine (150 μL of a 14.7 mM solution) and the buffer to initiate the reaction. The reaction was monitored by observation of spectrophotometric changes in the combined spectrum of the two reactants using a Varian Cary 3 spectrophotometer. The reaction was deemed complete when spectrophometric changes ceased. The sample was then removed from the cuvette and loaded onto the semipreparative 21.2 mm × 250 mm Synergi 10 μm polar-RP phenyl column (Phenomenex) run isocratically at 4 mL/min in 10 mM sodium phosphate buffer (pH 2.5) and 1% acetonitrile. The partially purified products were collected and dried under vacuum before being dissolved in water (5% D_2O) and examined using ^{1}H NMR. The reaction mixture was also studied using an Agilent 1100 series LC−/MS system. Twenty microliters of the reaction mixture was chromatographed using a 4.6 mm × 150 mm, 5 μm Xterra C18 column (Waters) run isocratically at 0.8 mL/min in 10 mM ammonium formate and 1% acetonitrile (pH 3.2). All masses were recorded in negative ion mode.

Inhibition Studies of SaHPPD N245S. To demonstrate the extent to which the SaHPPD N245S variant is susceptible to inhibition by NTBC, the kinetics of formation of the metal to ligand charge-transfer absorption band of the HPPD·Fe(II)·NTBC complex were observed. These experimental methods parallel those reported for the WT enzyme (*23*). A Hi-Tech (now TgK) Scientific stopped-flow spectrophotometer (model 61-DX2) was used to measure the accumulation of the charge-transfer absorbance that occurred with mixing of anaerobic SaHPPD N245S·Fe(II) (final concentration of 47.5 μM) with pseudo-first-order concentrations of NTBC (final concentration ranging from 370 to 5825 μM). Solutions of NTBC were made anaerobic by being sparged with argon for 10 min prior to being loaded onto the stopped-flow apparatus. The instrument was maintained at 7 °C throughout the experiment. Data were collected from 2.15 ms to 20 s at 450 nm. The data were fit to eq 1, a linear combination of two exponentials

$$A_{450} = A_1(e^{-k_1 t}) + A_2(e^{-k_2 t}) + C \quad (1)$$

where A_1 and A_2 are the amplitudes of each phase and C is the absorbance end point of the trace. The dependence of the observed rate constant (k_1) for the more rapid phase was fit to eq 2 that describes a pre-equilibrium of an initial complex (dissociation constant, K_1) that does not have an absorbance contribution at 450 nm yet hyperbolically influences the rate constant observed in the first phase as a function of NTBC concentration. The dependence of the second phase on NTBC concentration was fit to a linear expression.

$$k_{obs} = k_1[\text{NTBC}]/(K_1 + [\text{NTBC}]) \quad (2)$$

NTBC inhibition of the *R. norvegicus* HPPD N241S variant was studied using a Hansatech Oxygraph dioxygen electrode. The reaction included 1 mM ascorbate, 15 μL of crude enzyme, 20 μM Fe(II), 250 μM HPP, and various NTBC concentrations in 20 mM HEPES (pH 7.0). Initially, the background rate of dioxygen consumption due to Fenton chemistry was established, after which the reaction was initiated by the addition of HPP. Inhibition was demonstrated by addition of concentrations of NTBC (2.5, 5, and 10 μM) 5 s after the initiation of the reaction with HPP. Each assay was monitored until the rate of dioxygen consumption returned to that measured for the background.

RESULTS

Expression and Purification. The WT and mutated genes for *S. avermitilis* and rat HPPDs were cloned into the pET17b plasmid which permitted heterologous expression in BL21(DE3) *E. coli*. Both proteins overexpressed satisfactorily; 0.1 mM IPTG was used to induce production of SaHPPD and SaHPPD N245S, but more activity accumulated for the rat enzymes when an extended incubation at a lower temperature without induction was used. The rat enzyme proved to be considerably less stable than the bacterial form, losing the bulk of the initially observed activity during standard salt fractionation steps. For this reason, we chose to center our investigations on the N to S variant from *S. avermitilis*. However, we verified that the key conclusions drawn from the bacterial context could be generalized to mammalian HPPDs (vide infra).

Principle Catalytic Observations. For the SaHPPD N245S variant, we find that the rate of O_2 consumption in response to the presence of HPP is similar to that of the well-studied wild-type enzyme (*22*). The measured kinetic parameters for the SaHPPD N245S variant show a k_{cat} of 4.6 ± 0.3 s^{-1} and a K_{mHPP} of 84 ± 17 μM. However, spectrophotometric changes that occur during

enzymatic turnover differ markedly from those of the WT enzyme and clearly show the evolution of a new product with a maximum at 226 nm (Figure 2). 1D ^{1}H NMR of the purified product material in D_2O shows a simple molecule, having only three ^{1}H resonances, two downfield doublets and one singlet in the aliphatic region. Each of these resonances has equivalent integration values. The same spectrum was obtained in a 5% D_2O/95% H_2O mixture with WATERGATE solvent suppression, ruling out any missing exchangeable proton resonances. The chemical shifts observed [^{1}H NMR (D_2O) δ 7.03 (2H, d, J = 10.2 Hz), 6.14 (2H, d, J = 10.2 Hz), 2.53 (2H, s)] are in good agreement with those previously reported for QAA in acetone-d_6 (*24*) and 1D ^{13}C spectra, and HMBC and HSQC cross-peaks further support this conclusion [^{13}C NMR (D_2O) δ 189.001, 177.547, 153.336, 127.350, 68.335, 47.295]. Moreover, LC−MS indicates a product with a mass of 167.1 corresponding to the mass of the quinolacetate ion (Figure S2 of the Supporting Information). Despite the fact that this variant enzyme does not produce homogentisate as its primary product, it is an efficient catalyst converting 96% of the added HPP to QAA. We therefore conclude that the principle product of this N to S HPPD variant is QAA (Figure 2). The potential mechanistic implications of the formation of this product are summarized in Scheme 2 and will be addressed further in Discussion (vide infra).

Coupling of Quinolacetic Acid to Thiols. Quinolacetic acid is a reactive dienone that is expected to be prone to Michael addition with intracellular thiols. Hawkinsin is one two-electron reduction reaction from the expected product of QAA and cysteine addition (Scheme 1), or one reductive step and one hydrolysis step away from the predicted product of glutathione addition. When we mixed purified QAA with L-cysteine in an anaerobic environment, an extinction coefficient change of ~800 M^{-1} cm^{-1} was observed at 250 nm (Figure S2 of the Supporting Information). These changes exhibited a half-life of approximately 400 s, suggesting that the net second-order rate constant for the reaction is ~1.2 M^{-1} s^{-1} (inset of Figure S1 of the Supporting Information). As judged by NMR, HPLC, and LC−MS, the product of the reaction was a mixture of similar species. The NMR (500 MHz, 5% D_2O, WATERGATE) spectrum of the reaction without further purification showed four new doublets at fields below 5 ppm, and a complex overlap of multiplets between 2.3 and 4.0 ppm. Reverse phase HPLC separation resolved the mixture into three fractions, but none of these were pure. These fractions were lyophilized and dissolved in 5% D_2O. ^{1}H NMR spectra indicate that the components are distinct as they exhibit differing patterns of multiplets between 5−7 and 2−4 ppm. These components each show a mass of 288.0 by LC−MS, corresponding to the doubly deprotonated adduct (Figure S2 of the Supporting Information) (the predicted mass of the hawkinsin dianion is 289.3). A number of similar adducts could logically be expected to occur as a result of Michael addition. The C2 ring atom that is the site of cysteine addition would become chiral in the adduct, resulting in a racemic mixture of cis and trans forms. Second, both resulting enantiomers would be expected to be involved in a keto−enol tautomer equilibrium at C3 and C4 of the ring. It is also conceivable that after Michael addition at C2 and enol−keto tautomerization at C3 and C4 a second Michael addition could occur at C6 of the ring, giving a di-adduct with two cysteinyl groups resulting in four possible configurations of the double adduct. A mass of 407.9 is observed by LC−MS, consistent with a trianionic product of this type (data not shown).

NTBC Inhibition of N to S Variants. NTBC has been shown to bind exceedingly tightly to wild-type HPPDs, eliminating enzymatic activity by forming a bidentate association with the active site ferrous iron (*25*, *26*). This complex, while not covalent, is virtually irreversible (*23*). The addition of NTBC to SaHPPD

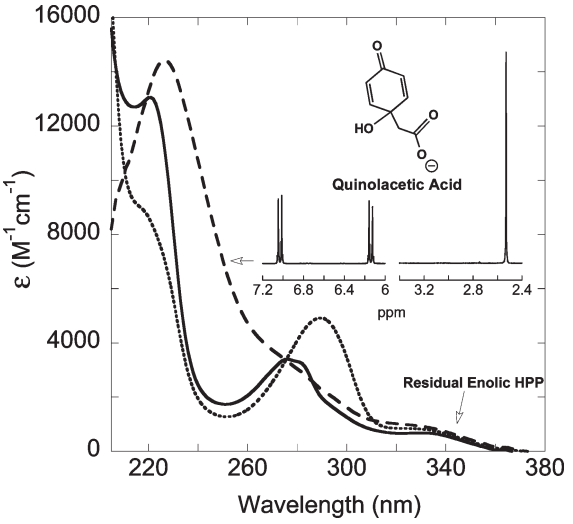

FIGURE 2: Identification of quinolacetic acid as the dominant product of the N to S mutation. The primary plot shows the absorption spectrum for HPP (—) compared to those of the products of wild-type HPPD, homogentisate (· · ·), and SaHPPD N245S, quinolacetic acid (− − −). The inset shows the 500 MHz NMR spectrum of the product of the SaHPPD N245S enzyme at ~2 mM in 99% D_2O.

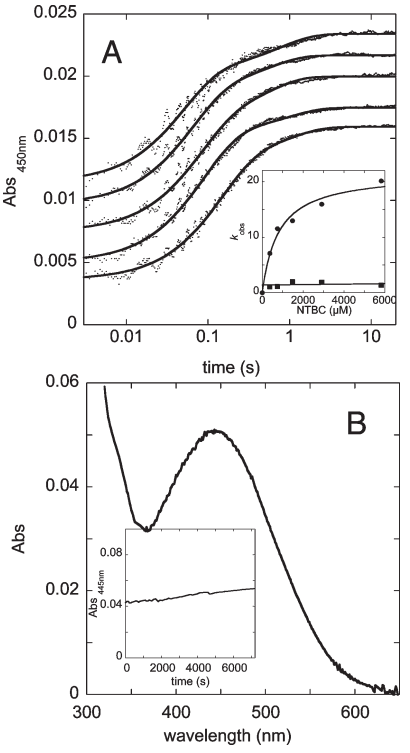

FIGURE 3: SaHPPD·NTBC Complex. (A) Kinetics of the accumulation of charge-transfer absorption bands arising from the SaHPPD N245S·NTBC complex. The anaerobic SaHPPD N245S·Fe(II) complex (final concentration of 47.5 μM) was mixed with anaerobic NTBC solutions that gave final concentrations of 370, 740, 1480, 2960, and 5825 μM. Traces are shown with increasing ligand concentration from bottom to top and were offset on the y-axis for the sake of clarity. Each trace was fit to a two-exponential model, and fits are depicted as solid lines. The inset shows the dependence of k_1 on NTBC concentration fit to a hyperbolic model according to eq 2 and k_2 fit to a straight line with a slope of zero. (B) Spectrum of the charge-transfer band of the SaHPPD N245S·NTBC complex. The inset shows the stability of the CT band when exposed to an O_2-containing atmosphere.

Scheme 2: Mechanistic Implications of the N to S Mutation

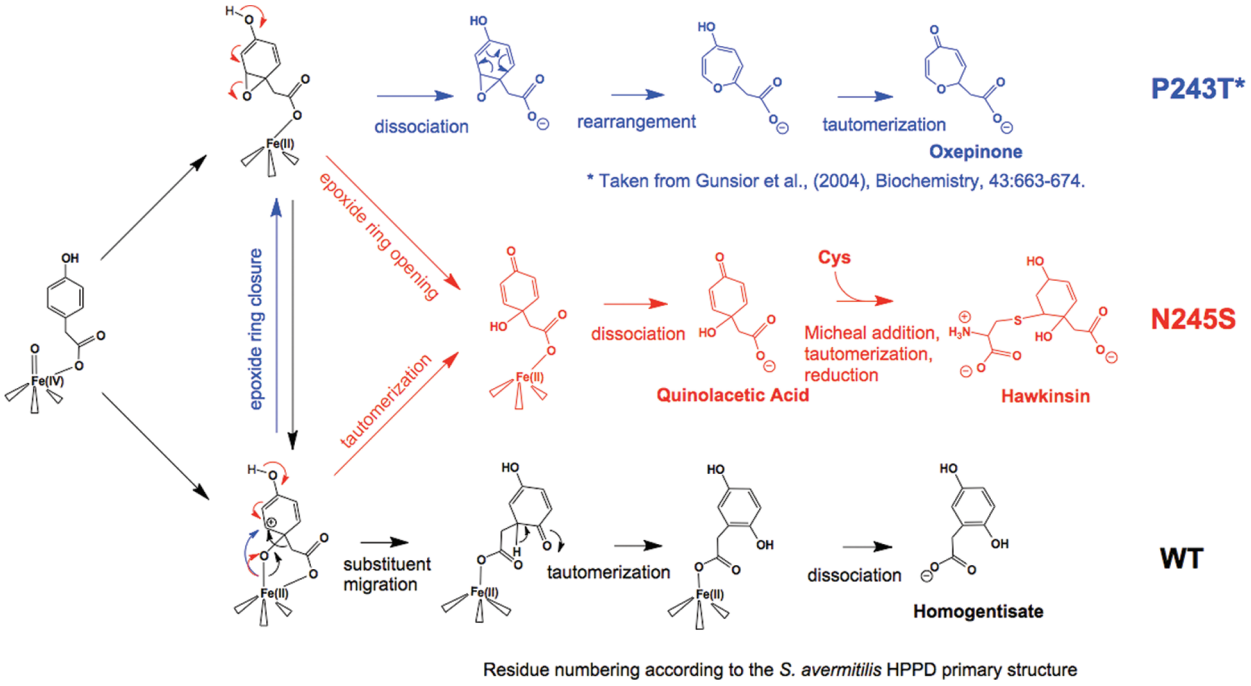

N245S likewise removes enzymatic activity. When NTBC was added at a ratio that was 1.1-fold greater than the concentration of SaHPPD N245S, the rate of O_2 consumption in the presence of HPP was reduced by ~97%, indicating tight stoichiometric binding. Similarly, the binding of NTBC to SaHPPD N245S produced metal to ligand charge-transfer transitions centered around 445 nm (Figure 3B) with an extinction coefficient maximum of 290 M^{-1} cm^{-1}. Moreover, when the SaHPPD N245S·NTBC complex (1:1) was exposed to air, this charge-transfer feature was not observed to diminish over the course of 66 h. Since it is known that NTBC binds only to the ferrous form of HPPD (*23*) and that the unliganded holoenzyme is highly prone to being oxidized to form the inactive ferric state, the persistence of the inhibitor charge-transfer complex in air indicates that the dissociation rate constant for NTBC is exceptionally small such that there is little or no opportunity for the enzyme to oxidize.

The onset of inhibitor complex charge-transfer absorption has been studied via stopped-flow spectrophotometry under anaerobic conditions, for the WT HPPDs (*23*, *27*), for the related enzyme, hydroxymandelate synthase (*28*), and now for the SaHPPD N245S variant (Figure 3A). Kinetic data were acquired near the peak absorption wavelength for the charge-transfer band at varying pseudo-first-order concentrations of NTBC. The kinetics of NTBC association can be fit to two spectrally observable steps. The faster phase accounts for 75% of the total amplitude change, and the observed rate constant for this step shows a hyperbolic dependence on NTBC concentration whose asymptote is 22.7 ± 1.5 s^{-1} (Figure 3B, inset). The equilibrium constant implied by the dependence is 0.79 ± 0.17 mM and suggests a weakly associated initial complex that does not induce charge transfer. The slower phase appears to be independent of NTBC concentration and has a rate constant k_3 of 1.49 ± 0.43 s^{-1}. These observations are consistent with a three-step model in which the first step is a spectrophotometrically silent pre-equilibrium giving rise to the hyperbolic nature of the dependence of the subsequent colored step. This model is ostensibly the same as that observed for wild-type SaHPPD, suggesting that the N245S variant is as subject to inhibition as the wild-type form and that the mutation does not change the binding mechanism significantly.

Observations for Rat HPPD N241S. To demonstrate that the observations made with the bacterial HPPD variant can be extended to mammalian forms of HPPD, two key observations were repeated with HPPD from rat (that is 89% identical to HPPD from human). First, the RnHPPD N241S variant was shown to evolve a dominant product by HPLC that coeluted with QAA produced from the SaHPPD N245S protein (Figure 4A). This product eluted 1 min ahead of HG that was evolved from the wild-type rat enzyme reacting with HPP. These observations strongly suggest that the product of the rat variant is the same as that from the *S. avermitilis* variant, QAA, and that the N to S mutation is indeed the causative mutation for Hawkinsinuria. Second, NTBC was used to halt the catalytic activity of RnHPPD N241S. For a crude preparation of the RnHPPD variant, the rates of O_2 consumption in assays are markedly impacted by the addition of NTBC (Figure 4B). The rate of oxygen usage returns to the nonenzymatic background rate within a few seconds of addition of micromolar amounts of the inhibitor. These results indicate that the mammalian form of the N to S variant enzyme is similarly subject to inhibition by NTBC. Collectively, these data suggest that NTBC in all likelihood will be an effective therapeutic for treating Hawkinsinuria.

DISCUSSION

Motivated by the recent report of a Hawkinsinuria patient with an Asn to Ser missense mutation, we introduced mutations encoding the analogous amino acid change in the rat and *S. avermitilis* HPPD genes. The active site of hydroxyphenylpyruvate dioxygenase is formed by an eight-stranded β-barrel within a protein fold that is structurally categorized into the large superfamily of vicinal oxygen chelate proteins (*29*). The iron-liganding residues, two histidines and a glutamate, are on the first, fifth, and eighth β-strands, while the Asn that is the subject of this article is on the fourth β-strand (Figure 1). This Asn is completely conserved in all known HPPDs but not in other

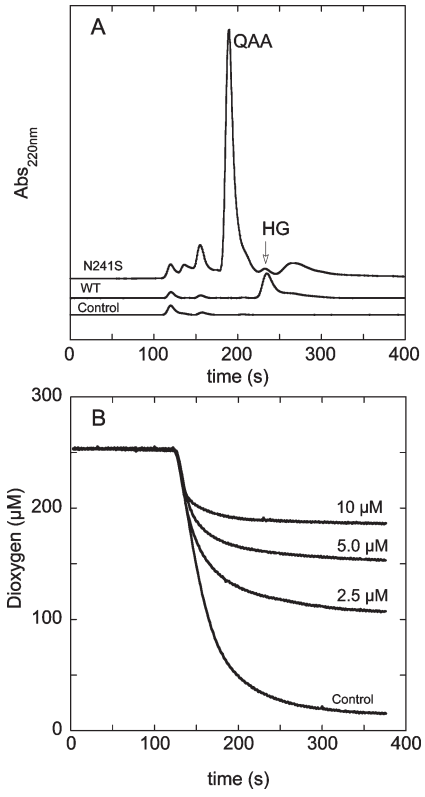

FIGURE 4: Product analysis and inhibition of a crude preparation of rat HPPD. (A) Product formation from HPP and dioxygen [75 μL of WT or RnHPPD N241S, 100 μM HPP, and 20 μM Fe^{2+} in 10 mM phosphate buffer (pH 7) at 25 °C]. The top trace is that of the QAA product with the RnHPPD A241S mutant, the middle trace that of the HG product with WT RnHPPD, and the bottom trace the control. (B) Onset of inhibition for the RnHPPD A241S mutant with differing concentrations of NTBC (as shown) in the presence of HPP as observed by dioxygen uptake. For each assay, HPP was added at 100 s and NTBC was added 5 s later.

mononuclear iron oxidoreductases of this fold, and not in the closely related enzyme hydroxymandelate synthase where it is universally an isoleucine (*30*). The involvement of this strand in positioning the phenol ring of the substrate and/or subsequent intermediates was evidenced by the results of mutating proline 243 to threonine in SaHPPD (*13*). This change to the strand resulted in a partitioning of products between the native product, HG, and the seven-membered oxepinone ring that was reasoned to have resolved from a 1,2-epoxide (Scheme 2). Molecular dynamics simulations of the substrate binding position, based on the hydroxymandelate synthase product complex structure, have indicated that the asparagine in question is likely involved in hydrogen bonding to the 4-hydroxyl group of HPP (Figure 1) (*31*). Given the absolute conservation of this amino acid and its structural position, it is not unexpected that there would be clinical significance to its mutation.

Both the rat and the *S. avermitilis* N to S enzyme variants yield QAA as the primary product. Because rat and human HPPDs are 89% identical, and *S. avermitilis* and human HPPDs are 47% identical (61% similar), the clinically observed enzyme variant of human HPPD almost certainly yields QAA. Though a patient whose gene is explicitly known to carry the N to S mutation has not been shown to excrete QAA (*7*), patients with Hawkinsinuria have been shown to excrete this molecule. Previously, this observation was rationalized as QAA arising from rearrangement of an epoxide product, but it is now known that the epoxide resolves instead as the oxepinone (*9*). HPPD is a member of the class of enzymes known as α-keto acid-dependent dioxygenases, where the O_2-dependent decarboxylation is thought to leave the enzyme in an Fe(IV)−oxo state, primed to add an oxygen atom to a proximal susceptible carbon atom. In HPPD, it is expected that the ensuing oxygenation results in the transient loss of the aromaticity of the ring to facilitate the 1,2 shift (NIH shift) of the aceto side chain to form HG (Scheme 2). For enzymes that exhibit NIH shifts, the nature of the intermediate that is formed after this oxygen atom adds has remained an open question for more than 40 years. A 1,2-epoxide or an arenium cation is most commonly proposed for reactions of this type (*32*−*37*), and these two species have the possibility of interconverting; therefore, finding evidence of one does not rule out the occurrence of the other during catalysis. The mechanistic implications of the N to S mutation and one other related mutation are summarized in Scheme 2. Earlier work by Gunsior et al. (*13*) showed that the P243T variant yields an oxepinone which implicates the involvement of an epoxide intermediate. However, the production of the QAA dienone by the N245S variant could just as readily imply an arenium cation species. Moreover, if the epoxide was released from the active site of the N245S variant, we would expect to see the oxepinone, and we do not [even at the elevated pH values used in the P243T study (*13*)]. Unfortunately, neither of the products made from these variant enzymes settles the issue of what intermediate is formed with oxygenation of the aromatic ring, nor do they establish the timing if both were to occur during the overall oxygenation reaction. It is clear, however, that both the P243T and N245S variants fail to hold the six-membered ring in a such a way as to induce the aceto substituent migration that leads to the native product, HG. Both abort after the second oxygen atom has been delivered and before the NIH shift (Scheme 2). It is also clear that the oxidation state of the metal ion at the moment at which the reaction aborts is 2+, at least for the N to S variant, as this enzyme is capable of many turnovers with HPP and dioxygen in the absence of a reducing agent. This observation narrows the mechanistic possibilities and is entirely consistent with the involvement of either an epoxide or benzylic cation, underscoring the fact that the nature of the NIH shift for HPPD is not substantially more elucidated by the observations made here. Nonetheless, the results presented in this work unequivocally show that the conserved asparagine altered in this study is intricately involved in the unique chemistry of HPPD, particularly the chemistry pertaining to the NIH shift of the aceto group. Moreover, given that the decarboxylation reaction is complete, we can confine the shift process to the latter half of the catalytic cycle.

Unlike the P243T variant of SaHPPD, with an activity decreased at least 20-fold from the wild-type value, the N245S variant has a k_{cat} (5 s^{-1}) very similar to that of the wild type (7 s^{-1}) and a k_{cat}/K_m (63 mM^{-1} s^{-1}) only 4-fold lower than that of the wild type (254 mM^{-1} s^{-1}). This observation has phenotypic implications for Hawkinsinuria and is no doubt responsible for reports of the autosomal dominant pattern of inheritance (*5*). Mutations that cause malady by rendering the gene product either absent, inactive, or largely inactive are more typically recessive, only presenting in the homozygote. The causative N to S variant for Hawkinsinuria would be expected to present the excretion of hawkinsin in all genotypes. Heterozygous individuals with a native second HPPD gene would be expected to have the more prevalent and more mild form of the disease. This genotype would occur in 50% of the offspring of Hawkinsinuria carriers, a fact that argues strongly both that the condition is vastly more common than the literature would indicate and that the heterozygote, while

impacted, may not exhibit sufficiently severe symptoms to prompt physicians to seek a diagnosis. The homozygous case would be predicted to cause the most debilitating form of the disease forming QAA and hence hawkinsin from both HPPDs expressed in the diploid. In these patients, the entire flux through tyrosine catabolism would result in QAA production.

Moreover, the individual from which the causative mutation was identified was compound heterozygous and carried the mutation for type III tyrosinemia in the second copy of the HPPD gene, causing this gene product to be inactive. Presumably, this individual presented with more severe symptoms and was screened for this reason (*7*). These arguments are predicated on the belief that the excretion of hawkinsin accompanies the symptoms of Hawkinsinuria. In truth, the etiology of Hawkinsinuria is not completely understood. It is not clear that hawkinsin itself has any particular toxicity, or what actually is the causative chemical entity for the symptoms observed, nor is the extent to which these molecules can be tolerated clear. Still it is reasonable to presume that one of the byproducts of QAA or possibly QAA itself creates the pathology of Hawkinsinuria and that the severity of symptoms is linked to the concentration of this molecule.

Though NTBC was originally developed as a plant HPPD inhibitor for use as an agricultural herbicide, it has been used successfully to inhibit HPPD in type I tyrosinemia and alkaptanuria patients and is demonstrated to alleviate the symptoms of these diseases (neither of which arises from a HPPD mutation) (*20*, *21*). Importantly, for the treatment of Hawkinsinuria, the type 1 tyrosinemia therapy established that NTBC is well-tolerated by infants (*38*). Inhibiting HPPD, however, has the side effect of driving the first enzyme in the tyrosine catabolism pathway, tyrosine aminotransferase, toward the production of tyrosine and thereby increasing the blood tyrosine concentration. The effect of this can be localized tyrosine precipitation most notably in the eye and suggests that a low-tyrosine diet would be prudent to limit this complication.

We have shown that the N to S HPPD variant apparently responsible for the symptoms of Hawkinsinuria produces QAA and that this enzyme is as susceptible to NTBC inhibition as the WT HPPD in vitro. As such, we propose that NTBC should block the production of QAA in patients with the N to S genetic defect and suggest it is a candidate therapeutic for the treament of Hawkinsinuria.

ACKNOWLEDGMENT

We extend our thanks to Patrick Anderson of the Water Institute at the University of Wisconsin—Milwaukee for his assistance operating the LC−MS system. Thanks are also due to Holger Forsterling from the Department of Chemistry and Biochemistry at the University of Wisconsin—Milwaukee for his aid in operating the NMR instruments.

SUPPORTING INFORMATION AVAILABLE

Kinetics of the reaction of QAA with cysteine and LC−MS data identifying the masses of the products of this reaction. This material is available free of charge via the Internet at http://pubs.acs.org.

REFERENCES

1. Moran, G. R. (2005) 4-Hydroxyphenylpyruvate dioxygenase. *Arch. Biochem. Biophys. 433*, 117–128.
2. Niederwieser, A., Matasovic, A., Tippett, P., and Danks, D. M. (1977) A new sulfur amino acid, named hawkinsin, identified in a baby with transient tyrosinemia and her mother. *Clin. Chim. Acta 76*, 345–356.
3. Danks, D. M., Tippett, P., and Rogers, J. (1975) A new form of prolonged transient tyrosinemia presenting with severe metabolic acidosis. *Acta Paediatr. Scand. 64*, 209–214.
4. Wilcken, B., Hammond, J. W., Howard, N., Bohane, T., Hocart, C., and Halpern, B. (1981) Hawkinsinuria: A dominantly inherited defect of tyrosine metabolism with severe effects in infancy. *N. Engl. J. Med. 305*, 865–868.
5. Borden, M., Holm, J., Leslie, J., Sweetman, L., Nyhan, W. L., Fleisher, L., Nadler, H., Lewis, D., and Scott, C. R. (1992) Hawkinsinuria in two families. *Am. J. Med. Genet. 44*, 52–56.
6. Lehnert, W., Stogmann, W., Engelke, U., Wevers, R. A., and van den Berg, G. B. (1999) Long-term follow up of a new case of hawkinsinuria. *Eur. J. Pediatr. 158*, 578–582.
7. Item, C. B., Mihalek, I., Lichtarge, O., Jalan, A., Vodopiutz, J., Muhl, A., and Bodamer, O. A. (2007) Manifestation of hawkinsinuria in a patient compound heterozygous for hawkinsinuria and tyrosinemia III. *Mol. Genet. Metab. 91*, 379–383.
8. Endo, F. (1998) [Hawkinsinuria]. *Ryoikibetsu Shokogun Shirizu 18*, 141–143.
9. Hocart, C. H., Halpern, B., Hick, L. A., and Wong, C. O. (1983) Hawkinsinuria: Identification of quinolacetic acid and pyroglutamic acid during an acidotic phase. *J. Chromatogr. 275*, 237–243.
10. Tomoeda, K., Awata, H., Matsuura, T., Matsuda, I., Ploechl, E., Milovac, T., Boneh, A., Scott, C. R., Danks, D. M., and Endo, F. (2000) Mutations in the 4-hydroxyphenylpyruvic acid dioxygenase gene are responsible for tyrosinemia type III and hawkinsinuria. *Mol. Genet. Metab. 71*, 506–510.
11. Niederwieser, A., Wadman, S. K., and Danks, D. M. (1978) Excretion of cis- and trans-4-hydroxycyclohexylacetic acid in addition to hawkinsin in a family with a postulated defect of 4-hydroxyphenylpyruvate dioxygenase. *Clin. Chim. Acta 90*, 195–200.
12. Ruetschi, U., Cerone, R., Perez-Cerda, C., Schiaffino, M. C., Standing, S., Ugarte, M., and Holme, E. (2000) Mutations in the 4-hydroxyphenylpyruvate dioxygenase gene (HPD) in patients with tyrosinemia type III. *Hum. Genet. 106*, 654–662.
13. Gunsior, M., Ravel, J., Challis, G. L., and Townsend, C. A. (2004) Engineering p-hydroxyphenylpyruvate dioxygenase to a p-hydroxymandelate synthase and evidence for the proposed benzene oxide intermediate in homogentisate formation. *Biochemistry 43*, 663–674.
14. O'Hare, H. M., Huang, F., Holding, A., Choroba, O. W., and Spencer, J. B. (2006) Conversion of hydroxyphenylpyruvate dioxygenases into hydroxymandelate synthases by directed evolution. *FEBS Lett. 580*, 3445–3450.
15. Dyson, J. S., Beulke, S., Brown, C. D., and Lane, M. C. (2002) Adsorption and degradation of the weak acid mesotrione in soil and environmental fate implications. *J. Environ. Qual. 31*, 613–618.
16. Sutton, P., Richards, C., Buren, L., and Glasgow, L. (2002) Activity of mesotrione on resistant weeds in maize. *Pest Manage. Sci. 58*, 981–984.
17. Secor, J. (1994) Inhibition of Barnyardgrass 4-Hydroxyphenylpyruvate Dioxygenase by Sulcotrione. *Plant Physiol. 106*, 1429–1433.
18. Kim, J.-S., Kim, T.-J., Kwon, O. K., and Cho, K. Y. (2002) Mechanism of Action of Sulcotrione, a 4-Hydroxyphenylpruvate Dioxygenase Inhibitor, in Developed Plant Tissues. *Photosynthetica 40*, 541–545.
19. Hall, M. G., Wilks, M. F., Provan, W. M., Eksborg, S., and Lumholtz, B. (2001) Pharmacokinetics and pharmacodynamics of NTBC (2-(2-nitro-4-fluoromethylbenzoyl)-1,3-cyclohexanedione) and mesotrione, inhibitors of 4-hydroxyphenyl pyruvate dioxygenase (HPPD) following a single dose to healthy male volunteers. *Br. J. Clin. Pharmacol. 52*, 169–177.
20. Lindstedt, S., Holme, E., Lock, E. A., Hjalmarson, O., and Strandvik, B. (1992) Treatment of hereditary tyrosinaemia type I by inhibition of 4-hydroxyphenylpyruvate dioxygenase. *Lancet 340*, 813–817.
21. Phornphutkul, C., Introne, W. J., Perry, M. B., Bernardini, I., Murphey, M. D., Fitzpatrick, D. L., Anderson, P. D., Huizing, M., Anikster, Y., Gerber, L. H., and Gahl, W. A. (2002) Natural history of alkaptonuria. *N. Engl. J. Med. 347*, 2111–2121.
22. Johnson-Winters, K., Purpero, V. M., Kavana, M., Nelson, T., and Moran, G. R. (2003) (4-Hydroxyphenyl)pyruvate Dioxygenase from *Streptomyces avermitilis*: The Basis for Ordered Substrate Addition. *Biochemistry 42*, 2072–2080.
23. Kavana, M., and Moran, G. R. (2003) Interaction of (4-hydroxyphenyl)pyruvate dioxygenase with the specific inhibitor 2-[2-nitro-4-(trifluoromethyl)benzoyl]-1,3-cyclohexanedione. *Biochemistry 42*, 10238–10245.

24. Saito, I., Yamane, M., Shimazu, H., Matsuura, T., and Cahnmann, H. J. (1975) Biogenetic Type Conversion of p-Hydroxyphenylpyruvic Acid into Homogentisic Acid. *Tetrahedron Lett. 9*, 641–644.
25. Brownlee, J., Johnson-Winters, K., Harrison, D. H. T., and Moran, G. R. (2004) The Structure of the Ferrous Form of (4-Hydroxyphenyl)pyruvate Dioxygenase from *Streptomyces avermitilis* in Complex with the Therapeutic Herbicide, NTBC. *Biochemistry 43*, 6370–6377.
26. Neidig, M. L., Decker, A., Kavana, M., Moran, G. R., and Solomon, E. I. (2005) Spectroscopic and computational studies of NTBC bound to the non-heme iron enzyme (4-hydroxyphenyl)pyruvate dioxygenase: Active site contributions to drug inhibition. *Biochem. Biophys. Res. Commun. 338*, 206–214.
27. Purpero, V. M., and Moran, G. R. (2006) Catalytic, noncatalytic, and inhibitory phenomena: kinetic analysis of (4-hydroxyphenyl)pyruvate dioxygenase from *Arabidopsis thaliana*. *Biochemistry 45*, 6044–6055.
28. Conrad, J. A., and Moran, G. R. (2008) The Interaction of Hydroxymandelate Synthase with the 4-Hydroxyphenylpyruvate Dioxygenase Inhibitor: NTBC. *Inorg. Chim. Acta 361*, 1197–1201.
29. Armstrong, R. N. (2000) Mechanistic diversity in a metalloenzyme superfamily. *Biochemistry 39*, 13625–13632.
30. He, P., Conrad, J. A., and Moran, G. R. (2010) The rate-limiting catalytic steps of hydroxymandelate synthase from *Amycolatopsis orientalis*. *Biochemistry 49*, 1998–2007.
31. Brownlee, J., He, P., Moran, G. R., and Harrison, D. H. (2008) Two roads diverged: The structure of hydroxymandelate synthase from *Amycolatopsis orientalis* in complex with 4-hydroxymandelate. *Biochemistry 47*, 2002–2013.
32. Moran, G. R., Derecskei-Kovacs, A., Hillas, P. J., and Fitzpatrick, P. F. (2000) On the Catalytic Mechanism of Tryptophan Hydroxylase. *J. Am. Chem. Soc. 122*, 4535–4541.
33. Guroff, G., Daly, J. W., Jerina, D. M., Renson, J., Witkop, B., and Udenfriend, S. (1967) Hydroxylation-induced migration: The NIH shift. *Science 157*, 1524–1530.
34. Jerina, D. M., Daly, J. W., and Witkop, B. (1968) The role of arene oxide-oxepin systems in the metabolism of aromatic substrates. II. Synthesis of 3,4-toluene-4-2H oxide and subsequent "NIH shift" to 4-hydroxytoluene-3-2H. *J. Am. Chem. Soc. 90*, 6523–6525.
35. Jerina, D. M., Daly, J. W., and Witkop, B. (1971) Migration of Substituents during Hydroxylation of Aromatic Substrates (NIH Shift). Oxidations with Peroxytrifluoroacetic Acid. *Biochemistry 10*, 366–372.
36. Daly, J. W., Jerina, D. M., and Witkop, B. (1972) Arene oxides and the NIH shift: The metabolism, toxicity and carcinogenicity of aromatic compounds. *Experientia 28*, 1129–1264.
37. Kasperek, G. J., Bruice, T. C., Yagi, H., and Jerina, D. M. (1972) Differentiation between the concerted and stepwise mechanisms for aromatization (NIH-shift) of arene epoxides. *J. Chem. Soc., Chem. Commun.,* 784–785.
38. McKiernan, P. J. (2006) Nitisinone in the treatment of hereditary tyrosinaemia type 1. *Drugs 66*, 743–750.